TORC1 Signaling Is Governed by Two Negative Regulators in Fission Yeast

Ning Ma,* Qingbin Liu,* Lili Zhang,* Elizabeth P. Henske,† and Yan Ma*,[1]

*Division of Molecular Pharmacology and Pharmacogenomics, Department of Biochemistry and Molecular Biology, Kobe University Graduate School of Medicine, Kobe 650-0017, Japan and †Division of Pulmonary and Critical Care Medicine, Department of Medicine, Brigham and Women's Hospital and Harvard Medical School, Boston, Massachusetts 02115

ABSTRACT The target of rapamycin (TOR) is a highly conserved protein kinase that regulates cell growth and metabolism. Here we performed a genome-wide screen to identify negative regulators of TOR complex 1 (TORC1) in *Schizosaccharomyces pombe* by isolating mutants that phenocopy Δ*tsc2*, in which TORC1 signaling is known to be up-regulated. We discovered that Δ*npr2* displayed similar phenotypes to Δ*tsc2* in terms of amino acid uptake defects and mislocalization of the Cat1 permease. However, Δ*npr2* and Δ*tsc2* clearly showed different phenotypes in terms of rapamycin supersensitivity and Isp5 transcription upon various treatments. Furthermore, we showed that Tor2 controls amino acid homeostasis at the transcriptional and post-transcriptional levels. Our data reveal that both Npr2 and Tsc2 negatively regulate TORC1 signaling, and Npr2, but not Tsc2, may be involved in the feedback loop of a nutrient-sensing pathway.

THE target of rapamycin (TOR) plays vitally important roles in regulating cell growth and metabolism. TOR interacts with several proteins to form two structurally and functionally distinct complexes named TOR complex 1 (TORC1) and 2 (TORC2) (Laplante and Sabatini 2009, 2012). In response to environmental cues, TORC1 controls cell growth and differentiation by coordinating diverse cellular processes including transcription, translation, and autophagy. Research on TORC1 has generated a model of the complex TOR signaling network (Huang and Manning 2009; Orlova and Crino 2010; Laplante and Sabatini 2012). In the regulation of TORC1 signaling, four major signals have been identified, namely growth factors (insulin, IGF, etc.), energy status (AMP/ATP ratio), oxygen levels, and nutrients (amino acids) (Laplante and Sabatini 2009, 2012). In mammals, the tuberous sclerosis complex 1 and 2 (TSC1-TSC2) serves as a key point of signal integration. The growth factors stimulate TORC1 signaling via PI3K–Akt/PKB-mediated phosphoinhibition of TSC2 (Inoki *et al.* 2002; Manning *et al.* 2002). The energy starvation inhibits TORC1 signaling via AMPK-dependent phosphoactivation of TSC2 (Inoki *et al.* 2003). Then, TSC2 negatively regulates TORC1 activity by converting GTP-bound Rheb (Ras homolog enriched in brain) into its inactive GDP-bound state (Inoki *et al.* 2003; Tee *et al.* 2003). The amino acids, in particular the branched-chain amino acid leucine, positively regulate TORC1. The TORC1 signaling remains sensitive to amino acid deprivation in *TSC2*$^{-/-}$ cells (Nobukuni *et al.* 2005), indicating that the activation of TORC1 by amino acids is independent of TSC2. Recently, it was demonstrated that TORC1 responds to amino acid availability via mechanisms involving Rag GTPases (Sancak *et al.* 2008). In the presence of amino acids, the Rag GTPases interact with TORC1, thereby promoting the translocation of TORC1 to the lysosomal membranes and facilitating Rheb's activation of TORC1 (Sancak *et al.* 2010).

In budding yeast *Saccharomyces cerevisiae*, *TOR1* and *TOR2* genes were originally identified as the targets of rapamycin, and mutations in *TOR1* or *TOR2* genes confer resistance to rapamycin (Heitman *et al.* 1991; Kunz *et al.* 1993). Studies using budding yeast have extensively enhanced our knowledge about TOR signaling; however, in this model there are no Tsc homologs. In contrast, in fission yeast *Schizosaccharomyces pombe*, Tsc1 and Tsc2 form a complex that acts as a GTPase activating protein (GAP) for the small GTPase Rhb1 (Rheb homolog) (van Slegtenhorst *et al.*

doi: 10.1534/genetics.113.154674
Manuscript received July 2, 2013; accepted for publication July 31, 2013
Supporting information is available online at http://www.genetics.org/lookup/suppl/doi:10.1534/genetics.113.154674/-/DC1.
[1]Corresponding author: Division of Molecular Pharmacology and Pharmacogenomics, Department of Biochemistry and Molecular Biology, Kobe University Graduate School of Medicine, 7-5-1 Kusunoki-cho, Chuo-ku, Kobe 650-0017, Japan. E-mail: mayan@med.kobe-u.ac.jp

2004; Nakase *et al.* 2006), and Rhb1 physically associates with Tor2 in a GTP-dependent manner (Urano *et al.* 2005; Uritani *et al.* 2006). Recently, Nakashima *et al.* (2010, 2012) demonstrate that, similar to mammalian mTORC1–S6K–S6, the TORC1 (Tor2)–Psk1–Rps6 constitutes a nutrient-dependent signaling pathway. Valbuena *et al.* (2012) demonstrate that the Rag GTPases Gtr1 and Gtr2 activate TORC1 in response to amino acids. These studies provide evidence that fission yeast is a valuable model to study the conserved Tsc–Rheb–TOR signaling network.

In the present study, we performed a genome-wide screen in *S. pombe* to identify the genes that inactivate Tor2 by isolating deletion mutants that phenocopy *tsc2* deletion. The Δ*npr2* cells displayed similar phenotypes to Δ*tsc2* cells in terms of the growth defect on normal Edinburgh minimal medium (EMM) plates supplemented with leucine, canavanine resistance, and Cat1 mislocalization. However, Δ*npr2* and Δ*tsc2* cells also showed several distinct phenotypes. Notably, upon rapamycin treatment, Isp5 transcriptional activity in Δ*npr2* cells showed a marked increase that reached a level nearly 40- to 50-fold greater than that observed in Δ*tsc2* or wild-type (wt) cells, whereas upon nitrogen depletion the increase in Δ*npr2* cells was significantly smaller than that observed in Δ*tsc2* or wild-type cells. Taken together, these results indicate that Tsc2 and Npr2 function differently as negative regulators of TORC1 signaling.

Materials and Methods

Strains, media, and genetic and molecular biology methods

The commercially available *S. pombe* nonessential gene haploid deletion strains (Kim *et al.* 2010) were purchased from Bioneer Corporation (http://pombe.bioneer.com/). The other strains used in this study are listed in Supporting Information, Table S1. The complete medium YPD (yeast extract–peptone–dextrose) and the minimal medium EMM have been described previously (Toda *et al.* 1996). YE plates (0.5% yeast extract, 3% glucose, 2% agar) are supplemented with 225 mg/liter adenine, histidine, leucine, uracil, and lysine to produce YES (yeast extract with supplements) plates. Gene disruptions are abbreviated by the gene preceded by Δ (for example, Δ*npr2*). Proteins are denoted by roman letters and only the first letter is capitalized (for example, Npr2).

Construction of Isp5 promoter reporter plasmids

Renilla luciferase was chosen as a reporter system, because it is minimally influenced by the level of ATP in living cells (Zhou *et al.* 2012). A 1038-bp DNA fragment in the 5′ flanking region of the *isp5*$^+$ gene was amplified by PCR primers (sense primer 3940, 5′-AAC TGC AGG GGA TTT CAA GTC GGC CGC-3′; antisense primer 3941, 5′-CCG CTC GAG TTT AAT TTT TTG TTT GAT GG-3′). The amplified products containing 1038-bp Isp5 promoter were subcloned into the *Pst*I/*Xho*I-digested pKB5878 (Zhou *et al.* 2012), a phRG(R2.2)-basic multicopy vector (Promega) that contains Renilla luciferase reporter gene. The resulting plasmid was registered as pKB8527 and used as Isp5 promoter reporter vector.

Real-time monitoring assays of Isp5 transcriptional activity

The Isp5 promoter activity was measured as described by Zhou *et al.* (2012) with minor modifications. Briefly, cells transformed with the reporter plasmid pKB8527 were cultured at 27° in EMM to mid-log phase and the optical density was adjusted to 0.3 at 660 nm. After incubation for 4 hr at 27°, 1 ml of cells was washed twice and resuspended in fresh EMM with or without NH_4Cl, respectively. A final 5 mM coelenterazine (Promega, no. S200A) was added into the cells. Rapamycin (Sigma-Aldrich) was added to a final concentration of 0.2 μg/ml from a stock solution of 0.2 mg/ml in methanol, and Torin1 (Tocris Bioscience) was added to a final concentration of 200 nM from a stock solution of 1 mM in DMSO. Emission of light was detected and reported as relative light units (RLUs) using a luminometer (AB-2350; ATTO, Tokyo).

Construction of chromosome-borne Cat1–GFP under the control of its own promoter

The *cat1*$^+$ gene was amplified by PCR with the genomic DNA of wild-type cells as a template. The sense primer was (3886) 5′-CGG GAT CCA TGT CCC ATA GCG ATT TTA ATA TGG-3′, and the antisense primer was (3887) 5′-CGG GAT CCG CGG CCG CCA CAG AAA ACC GAA CTG ATT TTC-3′. The amplified product containing the *cat1*$^+$ gene was digested with *Bam*HI, and the resulting fragment was subcloned into the *Bam*HI site of BlueScriptSK (+) (Stratagene). Then, a *Bam*HI/*Not*I fragment containing *cat1*$^+$ was ligated to the *Bgl*II/*Not*I site of the C terminus of the GFP carrying the S65T mutation (Heim *et al.* 1995). The expression of pREP1–Cat1–GFP complemented the canavanine-resistant phenotype of the Δ*cat1* cells (data not shown). To obtain the chromosome-borne C-terminally tagged Cat1–GFP under the control of its own promoter, the DNA fragment containing the Cat1–GFP and *ura4*$^+$ marker was integrated into the chromosome at the *cat1*$^+$ gene locus of KP456 by homologous recombination after digesting the plasmid with a restriction enzyme.

Construction of GFP–Atg8 under pREP41 promoter

The *atg8*$^+$ gene was amplified by PCR with the genomic DNA of wild-type cells as a template. The sense primer was (3956) 5′-CGG GAT CCA TG CGT TCT CAA TTC-3′, and the antisense primer was (3957) 5′-CGG GAT CCG CGG CCG CCT AAA AAG GAA ACA C-3′. The amplified product containing *atg8*$^+$ was digested with *Bam*HI/*Not*I, and ligated to the N terminus of the GFP carrying the S65T mutation under pREP41 promoter (Heim *et al.* 1995). For ectopic expression of proteins, we used the thiamine repressible *nmt1* promoter (Maundrell 1993). Expression was induced by growing the cells in EMM without thiamine.

Gene deletion

A one-step gene disruption by homologous recombination was performed (Rothstein 1983). The *cat1*::*ura4*$^+$ disruption was constructed as follows: The *Bam*HI fragment containing *cat1*$^+$ was subcloned into the *Bam*HI site of pGEM7Zf (Promega). Then, a *Sma*I fragment containing *ura4*$^+$ was inserted into the *Hinc*II site of the previous construct. The fragment containing the disrupted *cat1*$^+$ gene was transformed into KP456. Stable integrants were selected on media lacking uracil, and disruption of the gene was checked by genomic Southern hybridization (data not shown).

The *npr2*::*natMX*$_6$ disruption was constructed by the marker switching method (Hentges *et al.* 2005). The *natMX*$_6$ was amplified by PCR with *pFA6a-natMX*$_6$ as a template (Hentges *et al.* 2005). The sense primer was (MX4/6cassUP) 5′-GAC ATG GAG GCC CAG AAT AC-3′, and the antisense primer was (MX4/6cassDwn) 5′-TGG ATG GCG GCG TTA GTA TC-3′. The amplified product containing *natMX*$_6$ cassette was transformed into *npr2*::*KanMX*$_4$ cells and plated onto YES plates. The transformants were incubated at 27° for 1 day and replicated onto YES containing 100 μg/ml nourseothricin. The colonies were picked up, and tested for drug resistance. The cells that only showed nourseothricin resistance were registered as KP6366 (*h*$^-$ *npr2*::*natMX*$_6$).

Miscellaneous methods

The fluorescence microscopy images were recorded and processed as described previously (Ma *et al.* 2009). Real-time reverse transcription–PCR was performed as described previously (Ryuko *et al.* 2012; Zhou *et al.* 2012). Database searches were performed using Pombe community database Pombase (http://www.pombase.org). Cell extract preparation and immunoblot analysis were performed as described previously (Sio *et al.* 2005). Anti-phospho-Akt substrate (PAS) polyclonal antibodies (no. 9611) were purchased from Cell Signaling Technology. Anti-α-tubulin (B5-1-2) antibodies were purchased from Sigma.

Results

Cell growth-based genomic library screen for negative regulators of TORC1

In fission yeast, several lines of evidence have demonstrated that Tsc2 functions as GAP for the small GTPase Rhb1 (van Slegtenhorst *et al.* 2004, 2005; Urano *et al.* 2005; Nakase *et al.* 2006), and Rhb1 positively regulates Tor2 activity (Urano *et al.* 2005; Uritani *et al.* 2006). Based on these reports we reasoned that isolation of the mutant strains that phenocopy Δ*tsc2* cells will identify novel negative regulators of Tor2. It is demonstrated that Δ*tsc2* cells have defects in amino acid uptake, thus resulting in slow growth when combined with auxotrophic mutations or resistance to the toxic arginine analog canavanine (Matsumoto *et al.* 2002; van Slegtenhorst *et al.* 2004). Prior to the comprehensive screening, we compared the growth of wild-type with Δ*tsc2* cells auxotrophic for leucine, adenine, and uracil (Bioneer) (Kim *et al.* 2010). As shown in Figure 1A, the Δ*tsc2* cells grew equally as well as wild-type cells on YES plates. However, Δ*tsc2* cells failed to grow on normal EMM (5 g/liter NH_4Cl) media with amino acid supplements. It is demonstrated that poor nitrogen source rescued the growth defect by increasing amino acid permease expression (Weisman *et al.* 2005). This prompted us to investigate whether low NH_4Cl (0.5 g/liter) EMM media can rescue the growth defect of Δ*tsc2* cells. On low NH_4Cl EMM plates with amino acid supplements, the Δ*tsc2* cells grew as well as wild-type cells (Figure 1A), suggesting that the growth defect of Δ*tsc2* cells is caused by the defective amino acid uptake on normal EMM plates. Similarly, Δ*tsc2* cells auxotrophic for leucine (*leu1* Δ*tsc2*) failed to grow on normal EMM plates supplemented with leucine, but grew as well as wild-type cells auxotrophic for leucine (*leu1 wt*) on low NH_4Cl EMM plates supplemented with leucine (Figure 1B). These results indicate that the growth defect of Δ*tsc2* cells is mainly due to leucine auxotrophy. Consistently, it is demonstrated that *leu1-32* Δ*tsc2* failed to grow on PM media containing 40–200 μg/ml leucine (Matsumoto *et al.* 2002; Nakase *et al.* 2006). As reported previously (van Slegtenhorst *et al.* 2004; Nakase *et al.* 2006) and as shown in Figure 1C, the prototrophic Δ*tsc2* cells displayed canavanine resistance.

Based on the phenotypes of Δ*tsc2* under various genetic backgrounds, we performed genome-wide screens as follows. In the preliminary screen, 3004 deletion strains auxotrophic for leucine, adenine, and uracil were streaked on YES, normal, or low NH_4Cl EMM plates with amino acid supplements. The mutants that show low NH_4Cl rescued growth defect were selected for the second screen. In the second screen, the candidates auxotrophic for leucine, adenine, and uracil were mated with prototrophic wild-type cells to get leucine auxotrophic or prototrophic strains. The leucine auxotrophic strains were tested for growth on normal or low NH_4Cl EMM plates supplemented with leucine. The prototrophic strains were tested for growth on canavanine plates. Using the genome-wide screen, we isolated 13 deletion strains that phenocopy Δ*tsc2* cells. Here we will report the characterization of one of them, Npr2 (SPAC23H3.03c) encoding a protein of 409 amino acids that is highly similar to human NPRL2 (30.3% identity and 58.2% similarity) (Figure S1). The other genes will be described elsewhere.

The Δnpr2 and Δtsc2 displayed similar but distinct phenotypes

The Δ*npr2* cells showed similar phenotypes to Δ*tsc2* cells. First, the Δ*npr2* cells auxotrophic for leucine, adenine, and uracil failed to grow on normal EMM plates supplemented with appropriate amino acids (Figure 1A). Second, leucine auxotrophic Δ*npr2* cells failed to grow on EMM plates supplemented with leucine, and low NH_4Cl rescued the growth defect (Figure 1B). Third, prototrophic Δ*npr2* cells displayed canavanine resistance (Figure 1C).

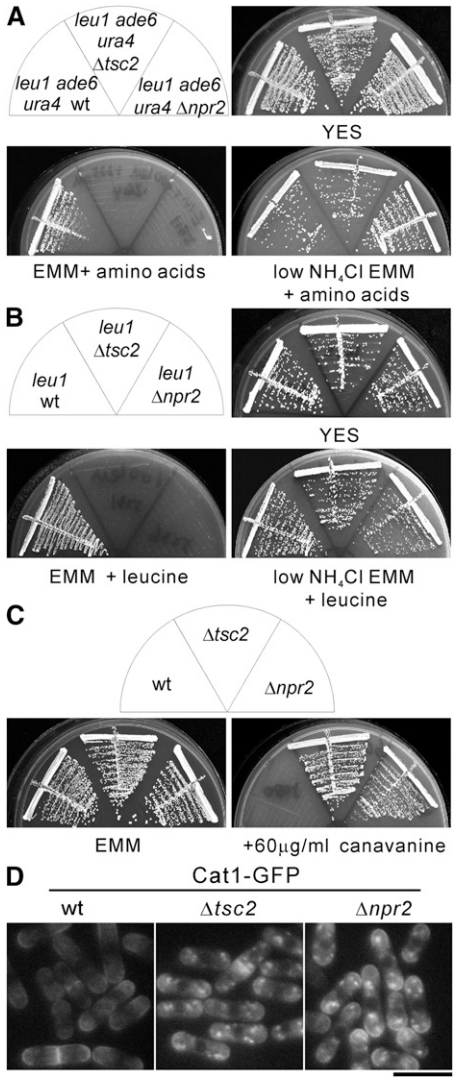

Figure 1 The Δ*npr2* and Δ*tsc2* cells display similar phenotypes. (A) The wild-type (KP93006), Δ*tsc2* (KP91087), and Δ*npr2* (KP90390) cells auxotrophic for leucine, adenine, and uracil were streaked onto YES, EMM (5 g/liter NH_4Cl), or low NH_4Cl EMM (0.5 g/liter NH_4Cl) supplemented with 100 mg/liter leucine, 225 mg/liter adenine, and 225 mg/liter uracil. The plates were incubated at 27° for 3 days (YES), 4 days (low NH_4Cl EMM + amino acids), or 5 days (EMM + amino acids), respectively. (B) The leucine auxotrophic cells of wild-type (HM123), Δ*tsc2* (KP5131), and Δ*npr2* (KP5236) were streaked onto YES, EMM (5 g/liter NH_4Cl), or low NH_4Cl EMM (0.5 g/liter NH_4Cl) supplemented with 100 mg/liter leucine. The plates were incubated as described in Figure 1A. (C) The prototrophic cells of wild-type (KP5080), Δ*tsc2* (KP5128), and Δ*npr2* (KP5237) were streaked onto EMM or EMM containing 60 μg/ml canavanine. The plates were incubated at 27° for 4 days (EMM) or 5 days (+60 μg/ml canavanine). (D) Subcellular localization of Cat1 in wild-type, Δ*tsc2*, and Δ*npr2* cells. The wild-type (KP5859), Δ*tsc2* (KP5826), and Δ*npr2* (KP5822) cells expressing chromosome-borne Cat1–GFP under the control of its own promoter were grown to early log phase in EMM media at 27°. The fluorescence of the Cat1–GFP was examined. Bar, 10 μm.

In fission yeast, the Tsc–Rhb1 signaling pathway controls basic amino acid uptake via the Cat1 permease, and Cat1 mislocalized into the intracellular organelles in Δ*tsc2* cells (Matsumoto *et al.* 2002). We constructed chromosome-borne Cat1–GFP under the control of its own promoter. We found that in wild-type cells, Cat1–GFP is mainly detected at the cell surface and is also enriched in the medial region and cell ends (Figure 1D). In Δ*npr2* and Δ*tsc2* cells, Cat1–GFP is localized to intracellular small punctuated structures and, to a lesser extent, to plasma membrane (Figure 1D). These results indicate that Δ*npr2* cells show very similar phenotypes to Δ*tsc2* cells.

To examine the genetic interaction between Tor2, Tsc2, and Npr2, we constructed *tor2-287*Δ*tsc2* and *tor2-287*Δ*npr2* double mutant cells and evaluated their temperature and rapamycin sensitivities as *tor2-287* is sensitive to temperature and rapamycin (Hayashi *et al.* 2007). Results showed that both *tor2-287*Δ*tsc2* and *tor2-287*Δ*npr2* double mutant cells displayed temperature- and rapamycin-sensitive phenotypes similar to *tor2-287* mutant cells (Figure 2A, bottom). Since the *tor2-287* mutation resulted in a rapamycin-sensitive phenotype, we expected that Δ*npr2* and Δ*tsc2* cells would show mild resistance to rapamycin. Unexpectedly, Δ*npr2* cells, but not Δ*tsc2* cells, showed supersensitivity to rapamycin. Similarly, Δ*npr2* and *tor2-287* cells, but not Δ*tsc2* cells, showed sensitivity to Torin1 (Figure 2A), which is a highly potent and selective ATP-competitive mTOR inhibitor (Thoreen *et al.* 2009).

Mutation or inhibition of Tor2 activity leads to canavanine resistance

We next examined the canavanine sensitivity of the *tor2-287* single mutant and *tor2-287*Δ*npr2* and *tor2-287*Δ*tsc2* double mutants. The results showed that the *tor2-287* mutant cells displayed canavanine resistance, and *tor2-287*Δ*npr2* and *tor2-287*Δ*tsc2* cells displayed similar canavanine resistance to the single mutant cells (Figure 2A, top). We confirmed that the expression of the $tor2^+$ gene under its endogenous promoter from a multicopy plasmid suppressed canavanine resistance of *tor2-287* mutant cells (Figure 2B), indicating that canavanine resistance is due to the *tor2* mutation. Consistently, Murai *et al.* (2009) demonstrated that another Tor2 allele, the *tor2-ts6* mutant, was resistant to canavanine.

Next, we examined several *tor2* point mutants in which the wild-type $tor2^+$ gene was replaced with a mutation on its chromosomal locus. The $tor2^{L1310P}$ and $tor2^{E2221K}$ mutants have activating mutations (Urano *et al.* 2007), and the $tor2^{S1837E}$ mutation has an inactivating mutation in the residue crucial for the binding between the FRB domain in TOR and the FKBP12–rapamycin complex (Nakashima *et al.* 2010). The inactivating $tor2^{S1837E}$ mutant, but not the activating mutant, displayed canavanine resistance (Figure 2C). Consistently, both rapamycin and Torin1 enhanced the canavanine resistance of wild-type cells (Figure 2C, wt).

Tor2 activity regulates transcription, intracellular trafficking, and protein level of Cat1

To examine whether canavanine resistance is due to the dysfunction of Cat1, a permease that transports arginine, we constructed a series of double mutants with Δ*cat1*. As shown

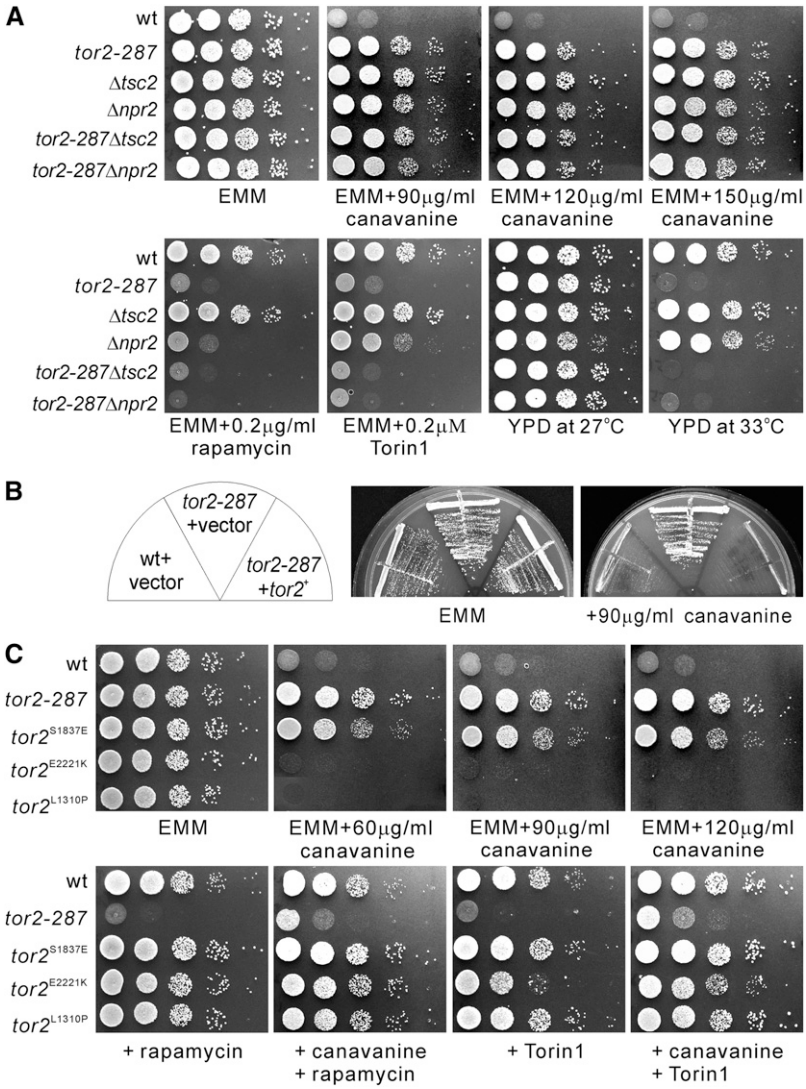

Figure 2 Tor2 dysfunction causes pleiotropic phenotypes. (A) Genetic interaction between Tor2, Tsc2, and Npr2. The *tor2-287* mutation caused pleiotropic phenotypes. The indicated single and double knockout cells were spotted onto the plates as indicated and then incubated for 3 days at 33° or 4–5 days at 27°. The cells were spotted in serial 10-fold dilutions starting with OD_{660} = 0.3 of log-phase cells (5 μl). (B) The *tor2*$^+$ gene rescued canavanine resistance of the *tor2-287* mutants. The *tor2-287* cells transformed with the control vector or the vector containing the *tor2*$^+$ gene were streaked onto the plates as indicated and then incubated for 4–5 days at 27°. (C) The phenotypes of *tor2* point mutation mutants. The indicated cells were spotted onto the indicated plates and incubated for 4–5 days at 27°.

in Figure 3A, *tor2-287*Δ*cat1* cells did not show synergism in resistance to canavanine compared with the parental single mutant cells, indicating that the *tor2-287* mutant displays canavanine resistance via Cat1. Notably, Δ*tsc2*Δ*cat1* and Δ*npr2*Δ*cat1* cells showed synergism in resistance to canavanine compared with the parental single knockout cells (Figure 3A), indicating Δ*tsc2* and Δ*npr2* displayed canavanine resistance not only via Cat1. To investigate whether the canavanine resistance in *tor2-287* cells is due to Cat1 mislocalization, we looked at the localization of Cat1 in *tor2-287* cells. The results showed Cat1 is prominently localized to plasma membrance (Figure 3B, *tor2-287*). In *tor2-287*Δ*npr2* cells, Cat1 showed similar localization as that observed in *tor2-287* cells (Figure 3B, *tor2-287*Δ*npr2*), suggesting that the *tor2* mutation rescued Cat1 mislocalization in *npr2* deletion background. Furthermore, our results show that low NH_4Cl rescued the mislocalization of Cat1 in Δ*npr2* and Δ*tsc2* cells (Figure 3C). We also noted that the fluorescence of Cat1–GFP in *tor2-287* cells was weaker compared to that observed in wild-type cells (Figure 3B). This prompted us to check the protein level of Cat1–GFP. The results revealed that the protein level of Cat1–GFP in *tor2-287* cells was lower than that in wild-type cells (Figure 3D). The two lower bands detected by immunoblot using anti-GFP antibody may represent protein degradation products of Cat1–GFP (Figure 3D, *1 and *2). Next, we examined the mRNA level of Cat1 using real time RT–PCR. In *tor2-287* cells, Cat1 mRNA level was significantly decreased compared with that in wild-type cells (Figure 3E), indicating that Tor2 positively regulates Cat1 transcription. Consistently, the Cat1 mRNA level in Δ*tsc2* and Δ*npr2* cells was slightly increased compared with that in wild-type cells (Figure 3E), suggesting a higher Tor2 activity in these cells even in normal EMM media. Based on these results, we hypothesize that Tor2 regulates Cat1 function at multiple steps, which may include transcription, membrane trafficking, and protein stability or degradation, and that Npr2 functions as a negative regulator of Tor2 (Figure 3F).

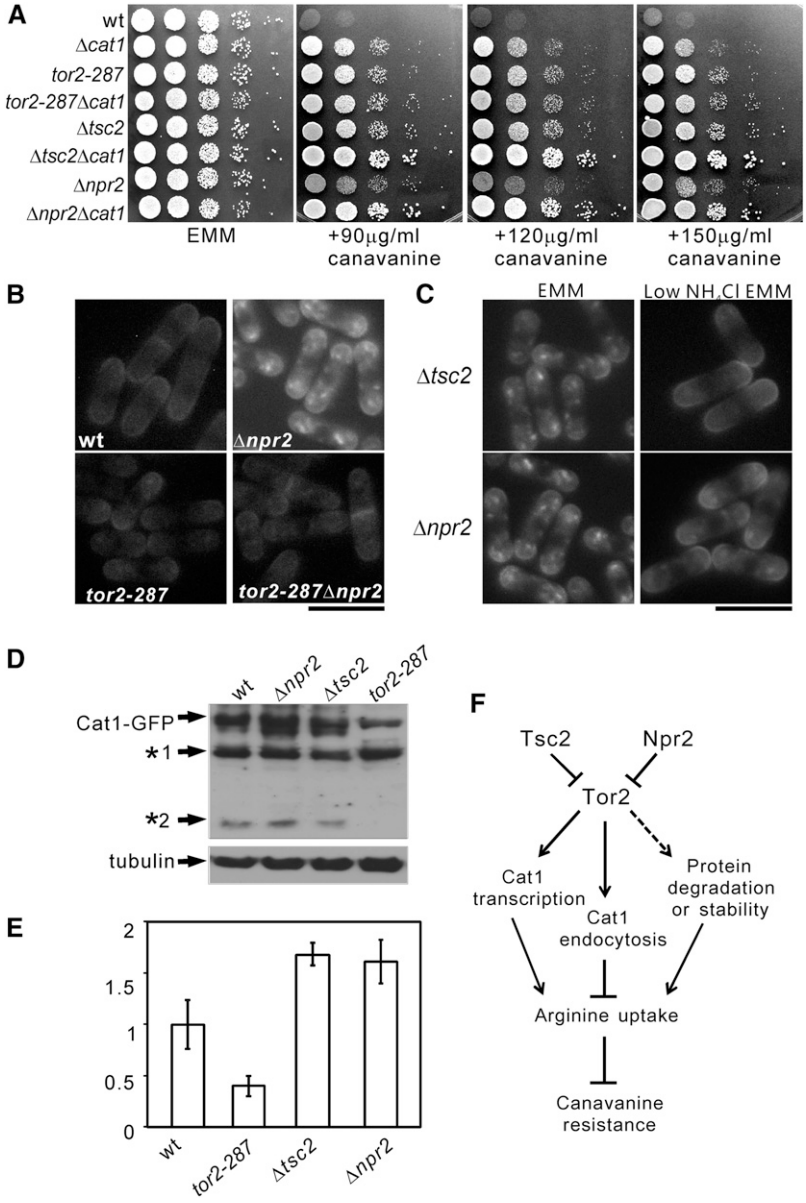

Figure 3 Tor2 signaling regulates Cat1 function. (A) The Δ*npr2*Δ*cat1* and Δ*tsc2*Δ*cat1* cells, but not *tor2-287*Δ*cat1* cells, were more resistant to canavanine compared with the parental single knockout cells. The indicated cells were spotted onto the plates as indicated and incubated for 4–5 days at 27°. (B) Subcellular localization of C-terminally tagged Cat1 in various cells. The wild-type (KP5859), *tor2-287* (KP5955), Δ*npr2* (KP5822), and *tor2-287*Δ*npr2* (KP6385) cells expressing chromosome-borne Cat1–GFP under the control of its own promoter were grown to early log phase in EMM media at 27°. The fluorescence was examined as described in Figure 1D. Bar, 10 μm. (C) Low NH_4Cl rescued Cat1 mislocalization in Δ*npr2* and Δ*tsc2* cells. The cells expressing chromosome-borne Cat1–GFP under the control of its own promoter were grown to early log phase in EMM media at 27° and divided into two aliquots. One aliquot was continued to be incubated in EMM, and the other aliquot was washed twice, and shifted to low NH_4Cl for 1 hr. The fluorescence was examined as described in Figure 1D. Bar, 10 μm. (D) The protein level of Cat1–GFP in various cells. The indicated cells were grown to early log phase in EMM media at 27° and then the cell extracts were subjected to electrophoresis using 8% polyacrylamide gel and were immunoblotted using anti-GFP antibodies to detect Cat1–GFP or using anti-α-tubulin antibodies to detect endogenous tubulin (loading control). *1 and *2 indicate possible degraded products of Cat1–GFP. (E) Tor2 activity affects Cat1 mRNA level. The indicated cells were grown overnight in EMM media to early log phase and then the cells were harvested. The RNA extract and real-time RT–PCR were performed as described in *Materials and Methods*. The data were analyzed by the comparative C_T method and were obtained from three independent experiments. (F) Working model illustrating the possible roles of Npr2, Tsc2, and Tor2 in canavanine resistance. Npr2 and Tsc2 function as negative regulators of Tor2. Tor2 affects Cat1 expression, membrane trafficking, and protein stability or degradation.

The Δnpr2 and Δtsc2 cells showed different phenotypes

In fission yeast, the expression of amino acid permease Isp5 is induced by the *tor2-ts6* mutation (Matsuo *et al.* 2007) and by the shift from EMM to proline media (Weisman *et al.* 2005). Deletion of the *tor1*$^+$ gene reduced the level of Isp5 expression (Weisman *et al.* 2005). We previously monitored transcriptional activity in living fission yeast cells using luciferase reporter genes (Deng *et al.* 2006; Zhou *et al.* 2010, 2012). Here we fused the native promoter of the *isp5*$^+$ gene with the Renilla luciferase reporter gene and estimated the activity of Tor2 using the Isp5–Renilla luciferase reporter system. Since Tor2 activation suppresses the transcription of Isp5 (Matsuo *et al.* 2007), and the shift from EMM to proline media induced Isp5 expression (Weisman *et al.* 2005), we expected that Tor2 inhibition by nitrogen depletion or rapamycin treatment should increase Isp5 transcriptional activity. The wild-type cells expressing the reporter vector were cultured and assayed as described in *Materials and Methods*. We found that in wild-type cells, Isp5 transcriptional activity was significantly induced by nitrogen depletion and Torin1 (Figure 4A, left). Nitrogen depletion and Torin1 treatment induced a 12- to 16- and a 6- to 10-fold increase in the ratio of accumulated RLU value up to 5 hr, respectively (Figure 4A, right). Notably, Isp5 transcriptional activity was not induced by rapamycin treatment (Figure 4A). Consistently, it was demonstrated that rapamycin treatment only led to subtle effects on gene expression, unless a poor nitrogen source was used (Rallis *et al.* 2013). In *tor2-287* cells, the reporter activity was significantly higher even in EMM media (data not shown), indicating that decreased Tor2 activity induced the transcription of Isp5.

Next we monitored the reporter activity in Δ*tsc2* and Δ*npr2* cells. In Δ*tsc2* cells, the level and pattern of reporter

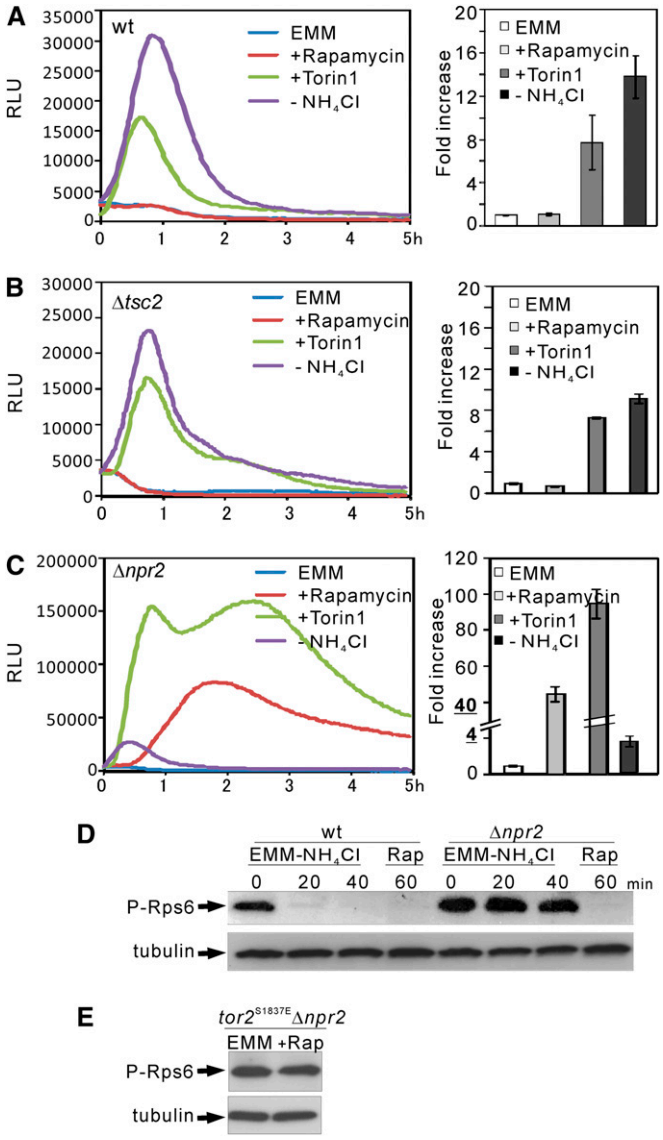

Figure 4 The Δ*npr2* and Δ*tsc2* cells show different phenotypes. (A) The transcriptional activity of the Isp5 promoter in wild-type cells. The wild-type cells harboring the reporter vector pKB8527 were grown to exponential phase and assayed as described in *Materials and Methods*. The luminescence was followed for 5 hr. The data shown are representative of multiple experiments. (Left) The luminescence, given as relative light units (RLUs), is plotted *vs.* time. (Right) The data represent the ratio of accumulated RLU value of each sample (nitrogen depletion, rapamycin treatment, or Torin1 treatment) to the basal (EMM). Standard deviations are from three independent experiments, and each sample was analyzed in triplicate. (B and C) The transcriptional activity of the Isp5 promoter in Δ*tsc2* and Δ*npr2* cells. The Δ*tsc2* or Δ*npr2* cells harboring the reporter vector pKB8527 were cultured and assayed as described in A. The data shown are representative of multiple experiments. (D) Nitrogen depletion-induced dephosphorylation of Rps6 is inhibited in Δ*npr2* cells. The prototrophic cells of wild-type (KP5080) and Δ*npr2* (KP5237) cells were grown at 27° to exponential phase in EMM (0 min). Then the cells were washed three times and transferred to liquid EMM-N for 20 and 40 min. Rapamycin was added to a final concentration of 0.2 μg/ml and incubated for 60 min in EMM media. The proteins were extracted as described in *Materials and Methods*. The cell lysates were subjected to SDS–PAGE and immunoblotted using anti-PAS polyclonal antibodies. Endogenous tubulin was immunoblotted using anti-α-tubulin antibodies as a loading control. (E) The effect of rapamycin was abolished in *tor2*^{S1837E}Δ*npr2* cells. Rapamycin treatment and immunoblot analysis was performed as described in D.

activity were almost the same as those observed in wild-type cells except that the nitrogen depletion-induced activity was slightly lower than that observed in wild-type cells (Figure 4B). Surprisingly, rapamycin treatment induced a 40- to 50-fold increase in Isp5 transcription in Δ*npr2* cells *vs.* a 1.1- to 1.4-fold increase in wild-type cells, while nitrogen depletion induced a 3.5- to 4.5-fold increase in Δ*npr2* cells *vs.* a 12- to 16-fold increase in wild-type cells (Figure 4, C *vs.* A). In Δ*fkh1*Δ*npr2* cells, Isp5 transcription activation induced by rapamycin was abolished, whereas that induced by Torin1 remained (Figure S2). This result is consistent with the finding that rapamycin inhibits Tor2 activity in an Fkh1-dependent manner, whereas Torin1 directly inhibits Tor2 activity. We also noted that in response to Torin1, the transcriptional activity in Δ*npr2* cells showed an initial activation followed by the second activation at 2–3 hr after the treatment. This profile differed significantly compared to that observed with Δ*tsc2* cells. These results suggest that several factors are involved in the Tor-dependent regulation of the Isp5 transcription profile, and they differentially affect the transcription profile.

Recent studies demonstrate that TORC1–Psk1–Rps6 constitutes a nutrient-dependent signaling pathway, and that the phosphorylation of Rps6 is a readout of Tor2 activity (Nakashima *et al.* 2010, 2012). We evaluated Rps6 phosphorylation in Δ*npr2* cells to test the role of Npr2 in regulating Tor2 activity. Rps6 phosphorylation is extremely high even after the shift to nitrogen-depletion media for 40 min, indicating that in Δ*npr2* cells, dephosphorylation of Rps6 upon nitrogen depletion is markedly inhibited. To address whether the elevated level of Rps6 phosphorylation in Δ*npr2* is due to the high activity of Tor2, we investigated the effect of rapamycin treatment on Rps6 phosphorylation. The results showed that Rps6 phosphorylation was completely abolished after rapamycin treatment for 60 min (Figure 4D). We also confirmed that in *tor2*^{S1837E}Δ*npr2* cells, rapamycin failed to decrease the elevated level of Rps6 phosphorylation (Figure 4E). Altogether, these results indicate that the elevated level of Rps6 phosphorylation in Δ*npr2* is due to the high activity of Tor2.

Npr2 negatively regulates Tor2 activity downstream of Rag GTPase

The results above strongly suggest that similar to Tsc2, Npr2 also negatively regulates Tor2 activity. To confirm the relationship between Npr2 and Tsc2, we analyzed the phenotypes of Δ*tsc2*Δ*npr2* double knockout cells. We found Δ*tsc2*Δ*npr2* cells did not exhibit synergism in resistance to canavanine, compared with the parental single knockout cells (Figure 5A). In terms of Torin1 and rapamycin sensitivities, Δ*tsc2*Δ*npr2* cells showed the same phenotypes as Δ*npr2* cells (Figure 5A). In Δ*tsc2*Δ*npr2* cells, rapamaycin-induced reporter activity is the same as that observed in Δ*npr2* cells (Figure 5B). In fission yeast, the Rag GTPases Gtr1 and Gtr2 activate Tor2 in response to amino acids (Valbuena *et al.* 2012). This prompted us to confirm the

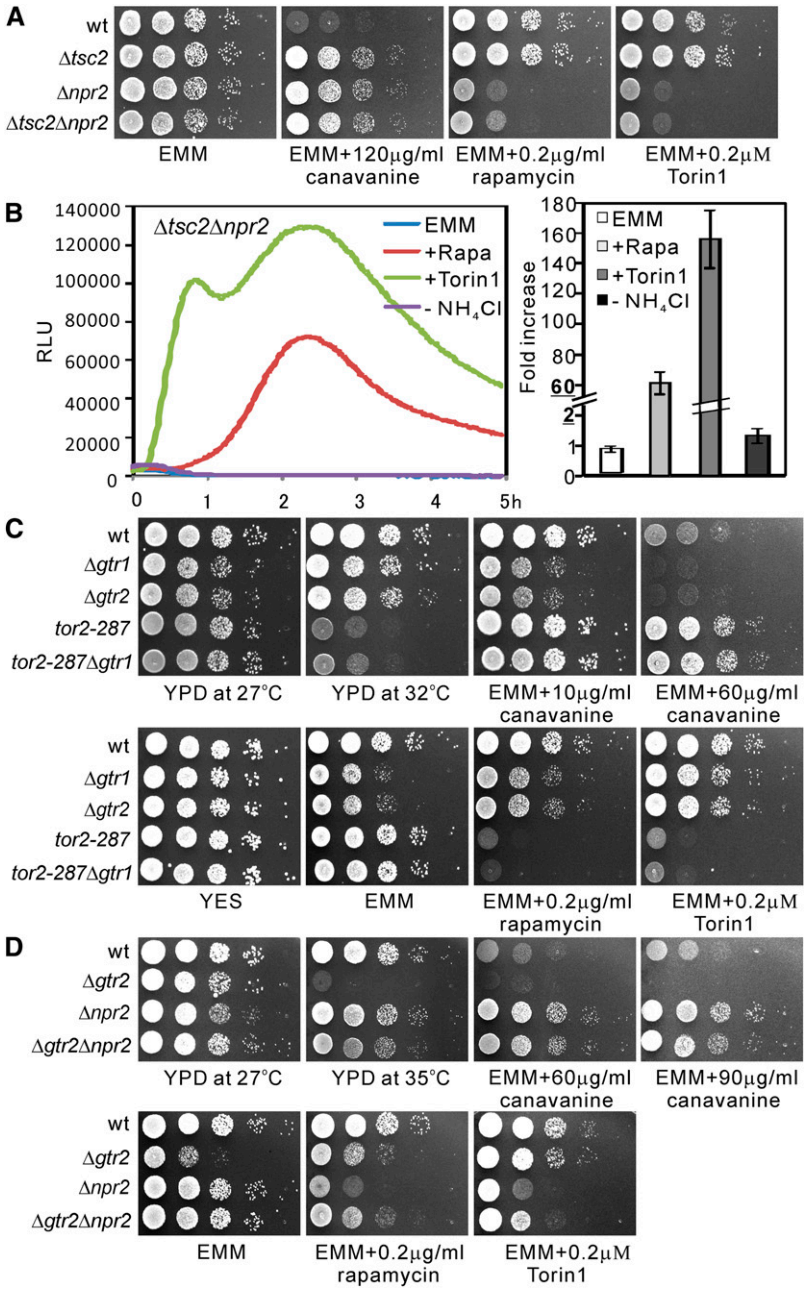

Figure 5 Genetic interaction between Npr2, Tsc2, and Gtr2. (A) The Δ*tsc2*Δ*npr2* double knockout cells display similar phenotypes to Δ*npr2* cells. The indicated cells were spotted onto the indicated plates and incubated for 4–5 days at 27°. (B) The Isp5 transcriptional activity was markedly increased in Δ*tsc2*Δ*npr2* double knockout cells in response to rapamycin and Torin1 treatment. The Δ*tsc2*Δ*npr2* cells harboring the reporter vector pKB8527 were grown and assayed as described in Figure 4A. (C) The *tor2-287*Δ*gtr2* double knockout cells displayed similar phenotypes to *tor2-287* cells. The indicated cells were spotted onto the indicated plates and incubated for 3 days at 32° or 4–5 days at 27°. (D) The Δ*gtr2*Δ*npr2* double knockout cells displayed similar phenotypes to Δ*npr2* cells. The indicated cells were spotted onto the indicated plates and incubated for 3 days at 35° or 4–5 days at 27°.

epistasis relationship between Tor2 and Gtr. The results showed Δ*gtr1* and Δ*gtr2* cells displayed the same phenotypes in terms of slow growth on EMM plates and mild sensitivity to canavanine (Figure 5C). The *tor2-287*Δ*gtr2* cells displayed the same phenotypes as *tor2-287* cells in terms of canavanine resistance, temperature-, rapamycin-, and Torin sensitivities (Figure 5C). These results indicate that Gtr2 functions upstream of Tor2. We next constructed Δ*npr2*Δ*gtr2* cells and investigated the relationship between Npr2 and Gtr2. The Δ*gtr2*Δ*npr2* cells displayed similar phenotypes to Δ*npr2* cells (Figure 5D), indicating that Npr2 may function downstream of Gtr2. Based on the *S. pombe* predicted protein interaction database (www.bahlerlab.info/PInt), Npr2 may interact with TORC1 subunits (Tor2, Toc1, and Tco89) and Gtr1–Gtr2–Vam6 complex with a score >0.5. Together with our genetic epistasis analyses data, we propose that Npr2 functions downstream of Gtr1–Gtr2 and upstream of Tor2.

The role of Npr2 in the regulation of autophagy

In budding yeast, *NPR2* deletion exhibited impaired autophagy induction (Wu and Tu 2011). In fission yeast, it is demonstrated that autophagy contributes to the maintenance of cell viability upon nitrogen depletion (Kohda *et al.* 2007). These reports prompted us to compare the growth of wild-type, Δ*tsc2*, and Δ*npr2* cells harboring the *leu1-32* mutation upon nitrogen deprivation on YES plates. As shown in Figure 6A, upon nitrogen deprivation for 30 min, the Δ*tsc2* and

Δ*npr2* grew as well as wild-type cells. Upon nitrogen deprivation for 6 hr, the growth of Δ*npr2* cells was significantly slower compared with that of wild-type and Δ*tsc2* cells. Upon nitrogen deprivation for 12 hr, the growth of both Δ*npr2* and Δ*tsc2* cells was markedly slower compared with that of wild type. Notably, the Δ*npr2* cells showed more a severe growth defect compared with Δ*tsc2* cells. These results suggest that Tor2 signaling plays a role in regulating autophagy. However, the cell viability experiment upon nitrogen deprivation does not appear to solely reflect autophagy. Then, we examined the cleavage of GFP–Atg8p, which is used to monitor autophagy in fission yeast (Mukaiyama *et al.* 2009, 2010), to test whether autophagy induction is affected in Δ*npr2* cells. As shown in Figure 6B, in wild-type cells, the cleavage from GFP–Atg8p to free GFP was detected upon nitrogen depletion for 4 hr. However, in both Δ*npr2* and Δ*tsc2* cells, the cleavage was markedly inhibited. These results indicate that Tor2 signaling plays a role in regulating autophagy.

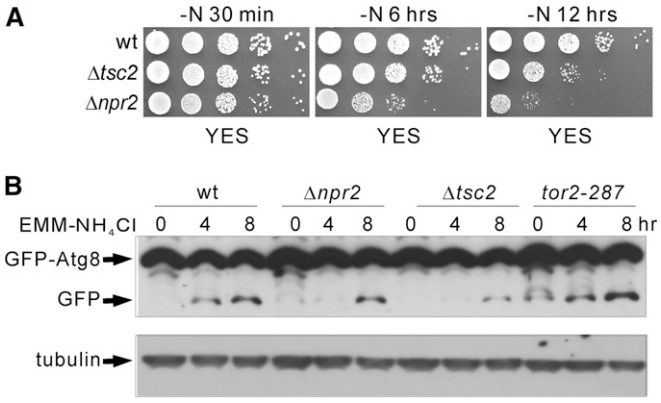

Figure 6 The role of Npr2 in the regulation of autophagy. (A) Viability of wild-type, Δ*tsc2*, and Δ*npr2* cells harboring the *leu1-32* mutation upon nitrogen deprivation. The indicated cells grown to logarithmic phase at 27° were collected, washed twice, and transferred to liquid EMM-N media. Aliquots of each culture were taken at the indicated time points, spotted onto YES plates in sequential 10-fold dilutions, and incubated at 27° for 3 days. (B) Cleavage of GFP–Atg8p. The multicopy plasmid encoding pREP41–GFP–Atg8p was introduced into the indicated cells. The transfomants were cultured in EMM to induce GFP–Atg8p expression. Then the cells were collected, washed three times, and transferred to liquid EMM-N media. Aliquots of each culture were taken at the indicated time points. The proteins were extracted as described in *Materials and Methods*. The cell lysates were subjected to SDS–PAGE and immunoblotted using anti-GFP antibodies. Endogenous tubulin was immunoblotted using anti-α-tubulin antibodies as a loading control.

Discussion

Fission yeast Npr2 and budding yeast Npr2p have similar but distinct functions

In budding yeast, Npr2p was first isolated as a **n**itrogen **p**ermeases **r**egulatory protein (Rousselet *et al.* 1995), and recently Npr2p was demonstrated to be a subunit of Npr2–Npr3 (Neklesa and Davis 2009), Iml1p–Npr2p–Npr3p (Wu and Tu 2011), and SEA (Sea1p/Imh1p–Sea2p–Sea3p–Sea4p–Npr2p–Npr3p) complexes (Dokudovskaya *et al.* 2011). The Npr2–Npr3 complex was identified in a genome-wide screen as negative regulators of TORC1 complex (Neklesa and Davis 2009). The Iml1p–Npr2p–Npr3p complex is required for nonnitrogen-starvation-induced autophagy (Wu and Tu 2011). The SEA (Seh1-associated) complex is a conserved coatomer-related complex that associates dynamically with the vacuoles (Dokudovskaya *et al.* 2011). In fission yeast, as shown in Table S2 Npr2 binds with five of the six components of SEA complex based on the predicted protein interaction database (www.bahlerlab.info/PInt).

Our present study is the first identification and functional analysis of Npr2 in fission yeast. Similar to budding yeast, fission yeast Npr2 also functions as a negative regulator of Tor2 based on several lines of genetic and biochemical evidence. First, Δ*npr2* cells failed to grow on leucine-supplemented EMM plates and showed canavanine resistance. Second, Δ*npr2* cells showed an increase in intracellular localization of Cat1. Third, in Δ*npr2* cells, Rps6 phosphorylation was extremely high even after the shift to nitrogen-depletion media for 40 min. Fourth, in Δ*npr2* cells, the cleavage of GFP–Atg8 was markedly inhibited. These four phenotypes may be a result of increased Tor2 activity in Δ*npr2* cells.

Despite these similarities, fission yeast Npr2 (SpNpr2) has two important differences from budding yeast Npr2p (ScNpr2p). First, ScNpr2p, but not SpNpr2, contains two characteristic PEST sequences, which are preferentially found in rapidly degraded regulatory proteins (Rousselet *et al.* 1995). Second, in budding yeast, deletion of ScNpr2p did not display rapamycin sensitivity (Wu and Tu 2011), whereas in fission yeast deletion of SpNpr2 resulted in rapamycin sensitivity.

Tsc2 and Npr2 play different roles in the regulation of Tor2 activity

We have shown that both Tsc2 and Npr2 function upstream of Tor2. One of the key questions that can be addressed in fission yeast, but not in budding yeast, is to list the differences between Δ*tsc2* and Δ*npr2* cells. First, Δ*npr2* cells displayed rapamycin sensitivity, whereas Δ*tsc2* cells did not. Second, rapamycin treatment induced a marked increase in Isp5 transcription in Δ*npr2* cells, whereas it failed to induce an increase in Δ*tsc2* cells. Third, nitrogen depletion induced less increase in Isp5 transcription in Δ*npr2* cells compared with Δ*tsc2* cells. These differences may be ascribed to differences in the level of Tor2 activation.

It is expected that an inhibitor would have less effect in the presence of high activity of its target, that is to say, Δ*tsc2* and Δ*npr2* cells should display less sensitivity to rapamycin due to increased Tor2 activity. Unexpectedly, rapamycin treatment induced an extremely marked increase in Isp5 transcriptional activity in Δ*npr2* cells, while no significant increase was observed in Δ*tsc2* or wild-type cells. Moreover, in Δ*tsc2* and wild-type cells Torin1 induced a marked increase in Isp5 transcriptional activity. The following mechanisms may be related to these effects of rapamycin and

Torin1. First, as an allosteric inhibitor, rapamycin inhibits TOR activity by forming the FKBP12–rapamycin complex that binds directly to the FRB domain of TOR (Huang *et al.* 2003). We hypothesize that rapamycin may inhibit TOR only in its activated state or only when TOR reaches a certain state of activation, thus rapamycin may have a more prominent effect in the cells that have high TOR activity. In mammalian and fission yeast cells, the effects of rapamycin on cell growth and proliferation are less severe than its effects in budding yeast (Weisman *et al.* 1997; Neshat *et al.* 2001; Takeuchi *et al.* 2005). These differences may be ascribed to differences in TOR activity. Second, as an ATP-competitive inhibitor, Torin1 inhibits both TORC1 and TORC2 in mammalian cells. It also inhibits many other kinases, although Torin1 was at least 200-fold selective for mTOR over other kinases (Thoreen *et al.* 2009). In mammalian cells, Torin1, but not rapamycin, mimics many phenotypes caused by TOR inhibition in budding yeast (Thoreen *et al.* 2009). Here, we report for the first time the effects of Torin1 on the growth and the transcriptional activity in fission yeast. Both Torin1 and rapamycin had similar effect on the growth inhibition of *tor2-287* mutant cells (Figure 2A), whereas Torin1, but not rapamycin, markedly induced Isp5 transcriptional activity (Figure 4A). These results suggest that the effects of Torin1 may also be explained by the inhibition of TORC1 and/or TORC2.

Our data demonstrate that Tsc2 and Npr2 function as negative regulators of Tor2 signaling in a parallel way, based on the following evidence: First, Δ*tsc2*Δ*npr2* cells showed the same phenotypes as Δ*npr2* cells in terms of rapamycin and Torin1 sensitivities, and the pronounced increase in Isp5 transcriptional activity response to the two TORC1 inhibitors. Second, Δ*gtr2*Δ*npr2* cells showed similar phenotypes to Δ*npr2* cells, indicating that Npr2 may function downstream of Gtr2. Consistently, *S. pombe* predicted protein interactions show Npr2 possibly interacts with TORC1 subunits and the Gtr1–Gtr2–Vam6 complex. In budding yeast, it is well established that the E3 ligase Rsp5 is required for the endocytosis of permeases (MacGurn *et al.* 2011). In fission yeast, the mislocalization of Cat1 in Δ*tsc2* cells was suppressed by the loss of the E3 ubiquitin ligase Rsp5 homolog, Pub1 (Aspuria and Tamanoi 2008). Based on our present study and previous work, we summarize our working model in Figure 7. We hypothesize that in fission yeast, Tor2 signaling regulates amino acid homeostasis by feedback mechanisms. First, Tor2 differently regulates the activity of multiple permeases at the transcriptional level. We found that Tor2 promotes Cat1 transcription and inhibits Isp5 transcription. This is consistent with the results in budding yeast that TOR promotes the activity of high-specificity amino acid permeases such as Tat2 and Hip1, and inhibits the synthesis and stability of the general amino acid permease Gap1 (Neufeld 2007). Second, Tor2 regulates Cat1 activity at the transcriptional and post-transcriptional levels. We hypothesize that the reduction in Tor2 activity decreased both Cat1 endocytosis and Cat1 transcription;

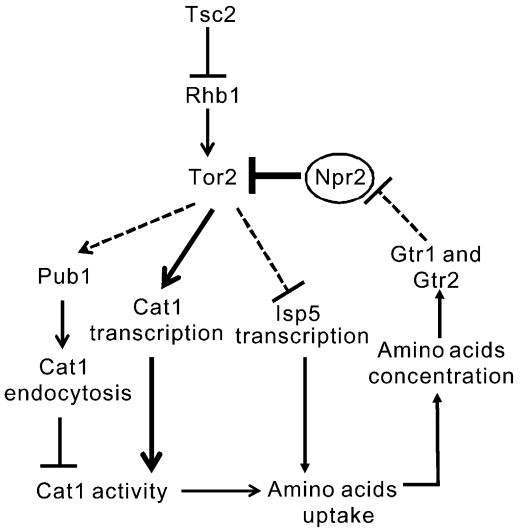

Figure 7 Working model for the role of Npr2 in regulating Tor2 signaling. In *S. pombe*, when Tor2 activity is increased in the presence of high intracellular amino acid, Pub1 is activated to prompt the endocytosis of permease Cat1, thus resulting in a decreased Cat1 activity. On the other hand, increased Tor2 activity inhibits the transcription of the permease Isp5. Both of these two changes result in decreased uptake of amino acids, thereby decreasing intracellular amino acid concentration. Gtr1 and Gtr2 sense the low amino acid levels and down-regulate Tor2 activity. In this feedback loop, Npr2 functions between Gtr1–Gtr2 and Tor2. In the absence of Npr2, Gtr1–Gtr2 fail to down-regulate Tor2 activity, thus resulting in a constitutively active Tor2 signaling. However, in the absence of Tsc2, the negative feedback loop is intact, thus resulting in partially active Tor2 signaling due to a relative high Rhb1 activity. The solid lines indicate the processes that are proven by other studies and the present study. The dashed lines indicate hypotheses that are not yet proven.

however, the effects on Cat1 transcription are stronger than those on Cat1 endocytosis. This may explain why the *tor2-287* mutant showed resistance to canavanine. Finally, increased Tor2 activity decreases the influx and level of amino acids, which in turn inhibits Tor2 activity, thus creating an autoinhibitory feedback loop that limits constitutive activation of Tor2 signaling. In this feedback loop, Npr2, but not Tsc2, appears to play key roles in the nutrient-sensing pathway that regulates amino acid homeostasis. Further studies are needed to elucidate the exact mechanisms through which Npr2 negatively regulates Tor2 signaling.

In mammalian cells, the tuberous sclerosis complex 1 and 2 (TSC1–TSC2) inhibits mTORC1. Treatment of human patients with TSC with rapamycin or rapamycin analogs results in a decrease in the size of kidney and central nervous system tumors by ∼30–40%, with regrowth to the original size when the treatment is discontinued (Henske and McCormack 2012). Our data in fission yeast point to the possibility that strategies focused on Npr2-dependent regulation of mTOR activity could contribute to more complete and/or more durable therapeutic responses for patients with TSC and lymphangioleiomyomatosis, and for other tumors with mTORC1 activation, including many human malignancies.

Acknowledgments

We thank Takayoshi Kuno for helpful advice and discussions. We thank Mitsuhiro Yanagida, Fuyuhiko Tamanoi, Sergio Moreno, Tomohiro Matsumoto, Antony M. Carr, and National BioResource Project for providing yeast strains and plasmids. We thank Akio Nakashima at Kobe University, and Nicole A. Neuman and Damir Khabibullin at Brigham and Women's Hospital and Harvard Medical School for helpful discussions and technical assistance. Financial support for this study was provided by Grant-in-Aid for Young Scientists (B) to Y.M. (no. 21790241) from the Japan Society for the Promotion of Science (http://www.jsps.go.jp/english/e-grants/grants.html).

Literature Cited

Aspuria, P. J., and F. Tamanoi, 2008 The Tsc/Rheb signaling pathway controls basic amino acid uptake via the Cat1 permease in fission yeast. Mol. Genet. Genomics 279: 441–450.

Deng, L., R. Sugiura, M. Takeuchi, M. Suzuki, H. Ebina *et al.*, 2006 Real-time monitoring of calcineurin activity in living cells: evidence for two distinct Ca^{2+}-dependent pathways in fission yeast. Mol. Biol. Cell 17: 4790–4800.

Dokudovskaya, S., F. Waharte, A. Schlessinger, U. Pieper, D. P. Devos *et al.*, 2011 A conserved coatomer-related complex containing Sec13 and Seh1 dynamically associates with the vacuole in Saccharomyces cerevisiae. Mol. Cell Proteomics 10: M110.006478.

Hayashi, T., M. Hatanaka, K. Nagao, Y. Nakaseko, J. Kanoh *et al.*, 2007 Rapamycin sensitivity of the *Schizosaccharomyces pombe tor2* mutant and organization of two highly phosphorylated TOR complexes by specific and common subunits. Genes Cells 12: 1357–1370.

Heim, R., A. B. Cubitt, and R. Y. Tsien, 1995 Improved green fluorescence. Nature 373: 663–664.

Heitman, J., N. R. Movva, and M. N. Hall, 1991 Targets for cell cycle arrest by the immunosuppressant rapamycin in yeast. Science 253: 905–909.

Henske, E. P., and F. X. McCormack, 2012 Lymphangioleiomyomatosis: a wolf in sheep's clothing. J. Clin. Invest. 122: 3807–3816.

Hentges, P., B. Van Driessche, L. Tafforeau, J. Vandenhaute, and A. M. Carr, 2005 Three novel antibiotic marker cassettes for gene disruption and marker switching in *Schizosaccharomyces pombe*. Yeast 22: 1013–1019.

Huang, J., and B. D. Manning, 2009 A complex interplay between Akt, TSC2 and the two mTOR complexes. Biochem. Soc. Trans. 37: 217–222.

Huang, S., M. A. Bjornsti, and P. J. Houghton, 2003 Rapamycins: mechanism of action and cellular resistance. Cancer Biol. Ther. 2: 222–232.

Inoki, K., Y. Li, T. Zhu, J. Wu, and K. L. Guan, 2002 TSC2 is phosphorylated and inhibited by Akt and suppresses mTOR signalling. Nat. Cell Biol. 4: 648–657.

Inoki, K., Y. Li, T. Xu, and K. L. Guan, 2003 Rheb GTPase is a direct target of TSC2 GAP activity and regulates mTOR signaling. Genes Dev. 17: 1829–1834.

Kim, D. U., J. Hayles, D. Kim, V. Wood, H. O. Park *et al.*, 2010 Analysis of a genome-wide set of gene deletions in the fission yeast *Schizosaccharomyces pombe*. Nat. Biotechnol. 28: 617–623.

Kohda, T. A., K. Tanaka, M. Konomi, M. Sato, M. Osumi *et al.*, 2007 Fission yeast autophagy induced by nitrogen starvation generates a nitrogen source that drives adaptation processes. Genes Cells 12: 155–170.

Kunz, J., R. Henriquez, U. Schneider, M. Deuter-Reinhard, N. R. Movva *et al.*, 1993 Target of rapamycin in yeast, TOR2, is an essential phosphatidylinositol kinase homolog required for G1 progression. Cell 73: 585–596.

Laplante, M., and D. M. Sabatini, 2009 mTOR signaling at a glance. J. Cell Sci. 122: 3589–3594.

Laplante, M., and D. M. Sabatini, 2012 mTOR signaling in growth control and disease. Cell 149: 274–293.

Ma, Y., M. Takeuchi, R. Sugiura, S. O. Sio, and T. Kuno, 2009 Deletion mutants of AP-1 adaptin subunits display distinct phenotypes in fission yeast. Genes Cells 14: 1015–1028.

MacGurn, J. A., P. C. Hsu, M. B. Smolka, and S. D. Emr, 2011 TORC1 regulates endocytosis via Npr1-mediated phosphoinhibition of a ubiquitin ligase adaptor. Cell 147: 1104–1117.

Manning, B. D., A. R. Tee, M. N. Logsdon, J. Blenis, and L. C. Cantley, 2002 Identification of the tuberous sclerosis complex-2 tumor suppressor gene product tuberin as a target of the phosphoinositide 3-kinase/akt pathway. Mol. Cell 10: 151–162.

Matsumoto, S., A. Bandyopadhyay, D. J. Kwiatkowski, U. Maitra, and T. Matsumoto, 2002 Role of the Tsc1-Tsc2 complex in signaling and transport across the cell membrane in the fission yeast *Schizosaccharomyces pombe*. Genetics 161: 1053–1063.

Matsuo, T., Y. Otsubo, J. Urano, F. Tamanoi, and M. Yamamoto, 2007 Loss of the TOR kinase Tor2 mimics nitrogen starvation and activates the sexual development pathway in fission yeast. Mol. Cell. Biol. 27: 3154–3164.

Maundrell, K., 1993 Thiamine-repressible expression vectors pREP and pRIP for fission yeast. Gene 123: 127–130.

Mukaiyama, H., S. Kajiwara, A. Hosomi, Y. Giga-Hama, N. Tanaka *et al.*, 2009 Autophagy-deficient *Schizosaccharomyces pombe* mutants undergo partial sporulation during nitrogen starvation. Microbiology 155: 3816–3826.

Mukaiyama, H., M. Nakase, T. Nakamura, Y. Kakinuma, and K. Takegawa, 2010 Autophagy in the fission yeast *Schizosaccharomyces pombe*. FEBS Lett. 584: 1327–1334.

Murai, T., Y. Nakase, K. Fukuda, Y. Chikashige, C. Tsutsumi *et al.*, 2009 Distinctive responses to nitrogen starvation in the dominant active mutants of the fission yeast Rheb GTPase. Genetics 183: 517–527.

Nakase, Y., K. Fukuda, Y. Chikashige, C. Tsutsumi, D. Morita *et al.*, 2006 A defect in protein farnesylation suppresses a loss of *Schizosaccharomyces pombe tsc2*$^{+}$, a homolog of the human gene predisposing to tuberous sclerosis complex. Genetics 173: 569–578.

Nakashima, A., T. Sato, and F. Tamanoi, 2010 Fission yeast TORC1 regulates phosphorylation of ribosomal S6 proteins in response to nutrients and its activity is inhibited by rapamycin. J. Cell Sci. 123: 777–786.

Nakashima, A., Y. Otsubo, A. Yamashita, T. Sato, M. Yamamoto *et al.*, 2012 Psk1, an AGC kinase family member in fission yeast, is directly phosphorylated and controlled by TORC1 and functions as S6 kinase. J. Cell Sci. 125: 5840–5849.

Neklesa, T. K., and R. W. Davis, 2009 A genome-wide screen for regulators of TORC1 in response to amino acid starvation reveals a conserved Npr2/3 complex. PLoS Genet. 5: e1000515.

Neshat, M. S., I. K. Mellinghoff, C. Tran, B. Stiles, G. Thomas *et al.*, 2001 Enhanced sensitivity of PTEN-deficient tumors to inhibition of FRAP/mTOR. Proc. Natl. Acad. Sci. USA 98: 10314–10319.

Neufeld, T. P., 2007 TOR regulation: sorting out the answers. Cell Metab. 5: 3–5.

Nobukuni, T., M. Joaquin, M. Roccio, S. G. Dann, S. Y. Kim *et al.*, 2005 Amino acids mediate mTOR/raptor signaling through activation of class 3 phosphatidylinositol 3OH-kinase. Proc. Natl. Acad. Sci. USA 102: 14238–14243.

Orlova, K. A., and P. B. Crino, 2010 The tuberous sclerosis complex. Ann. N. Y. Acad. Sci. 1184: 87–105.

Rallis, C., S. Codlin, and J. Bahler, 2013 TORC1 signaling inhibition by rapamycin and caffeine affect lifespan, global gene expression, and cell proliferation of fission yeast. Aging Cell **12:** 563–573.

Rothstein, R. J., 1983 One-step gene disruption in yeast. Methods Enzymol. 101: 202–211.

Rousselet, G., M. Simon, P. Ripoche, and J. M. Buhler, 1995 A second nitrogen permease regulator in *Saccharomyces cerevisiae*. FEBS Lett. 359: 215–219.

Ryuko, S., Y. Ma, N. Ma, M. Sakaue, and T. Kuno, 2012 Genome-wide screen reveals novel mechanisms for regulating cobalt uptake and detoxification in fission yeast. Mol. Genet. Genomics 287: 651–662.

Sancak, Y., T. R. Peterson, Y. D. Shaul, R. A. Lindquist, C. C. Thoreen *et al.*, 2008 The Rag GTPases bind raptor and mediate amino acid signaling to mTORC1. Science 320: 1496–1501.

Sancak, Y., L. Bar-Peled, R. Zoncu, A. L. Markhard, S. Nada *et al.*, 2010 Ragulator-Rag complex targets mTORC1 to the lysosomal surface and is necessary for its activation by amino acids. Cell 141: 290–303.

Sio, S. O., T. Suehiro, R. Sugiura, M. Takeuchi, H. Mukai *et al.*, 2005 The role of the regulatory subunit of fission yeast calcineurin for *in vivo* activity and its relevance to FK506 sensitivity. J. Biol. Chem. 280: 12231–12238.

Takeuchi, H., Y. Kondo, K. Fujiwara, T. Kanzawa, H. Aoki *et al.*, 2005 Synergistic augmentation of rapamycin-induced autophagy in malignant glioma cells by phosphatidylinositol 3-kinase/protein kinase B inhibitors. Cancer Res. 65: 3336–3346.

Tee, A. R., B. D. Manning, P. P. Roux, L. C. Cantley, and J. Blenis, 2003 Tuberous sclerosis complex gene products, Tuberin and Hamartin, control mTOR signaling by acting as a GTPase-activating protein complex toward Rheb. Curr. Biol. 13: 1259–1268.

Thoreen, C. C., S. A. Kang, J. W. Chang, Q. Liu, J. Zhang *et al.*, 2009 An ATP-competitive mammalian target of rapamycin inhibitor reveals rapamycin-resistant functions of mTORC1. J. Biol. Chem. 284: 8023–8032.

Toda, T., S. Dhut, G. Superti-Furga, Y. Gotoh, E. Nishida *et al.*, 1996 The fission yeast *pmk1*$^+$ gene encodes a novel mitogen-activated protein kinase homolog which regulates cell integrity and functions coordinately with the protein kinase C pathway. Mol. Cell. Biol. 16: 6752–6764.

Urano, J., M. J. Comiso, L. Guo, P. J. Aspuria, R. Deniskin *et al.*, 2005 Identification of novel single amino acid changes that result in hyperactivation of the unique GTPase, Rheb, in fission yeast. Mol. Microbiol. 58: 1074–1086.

Urano, J., T. Sato, T. Matsuo, Y. Otsubo, M. Yamamoto *et al.*, 2007 Point mutations in TOR confer Rheb-independent growth in fission yeast and nutrient-independent mammalian TOR signaling in mammalian cells. Proc. Natl. Acad. Sci. USA 104: 3514–3519.

Uritani, M., H. Hidaka, Y. Hotta, M. Ueno, T. Ushimaru *et al.*, 2006 Fission yeast Tor2 links nitrogen signals to cell proliferation and acts downstream of the Rheb GTPase. Genes Cells 11: 1367–1379.

Valbuena, N., K. L. Guan, and S. Moreno, 2012 The Vam6 and Gtr1-Gtr2 pathway activates TORC1 in response to amino acids in fission yeast. J. Cell Sci. 125: 1920–1928.

van Slegtenhorst, M., E. Carr, R. Stoyanova, W. D. Kruger, and E. P. Henske, 2004 *Tsc1*$^+$ and *tsc2*$^+$ regulate arginine uptake and metabolism in Schizosaccharomyces pombe. J. Biol. Chem. 279: 12706–12713.

van Slegtenhorst, M., A. Mustafa, and E. P. Henske, 2005 Pas1, a G1 cyclin, regulates amino acid uptake and rescues a delay in G1 arrest in Tsc1 and Tsc2 mutants in Schizosaccharomyces pombe. Hum. Mol. Genet. 14: 2851–2858.

Weisman, R., M. Choder, and Y. Koltin, 1997 Rapamycin specifically interferes with the developmental response of fission yeast to starvation. J. Bacteriol. 179: 6325–6334.

Weisman, R., I. Roitburg, T. Nahari, and M. Kupiec, 2005 Regulation of leucine uptake by *tor1*$^+$ in *Schizosaccharomyces pombe* is sensitive to rapamycin. Genetics 169: 539–550.

Wu, X., and B. P. Tu, 2011 Selective regulation of autophagy by the Iml1-Npr2-Npr3 complex in the absence of nitrogen starvation. Mol. Biol. Cell 22: 4124–4133.

Zhou, X., Y. Ma, R. Sugiura, D. Kobayashi, M. Suzuki *et al.*, 2010 MAP kinase kinase kinase (MAPKKK)-dependent and -independent activation of Sty1 stress MAPK in fission yeast. J. Biol. Chem. 285: 32818–32823.

Zhou, X., Y. Ma, T. Kato, and T. Kuno, 2012 A measurable activation of the bZIP transcription factor Atf1 in a fission yeast strain devoid of stress-activated and cell integrity mitogen-activated protein kinase (MAPK) activities. J. Biol. Chem. 287: 23434–23439.

Communicating editor: J. Heitman

GENETICS

Supporting Information
http://www.genetics.org/lookup/suppl/doi:10.1534/genetics.113.154674/-/DC1

TORC1 Signaling Is Governed by Two Negative Regulators in Fission Yeast

Ning Ma, Qingbin Liu, Lili Zhang, Elizabeth P. Henske, and Yan Ma

DOI: 10.1534/genetics.113.154674

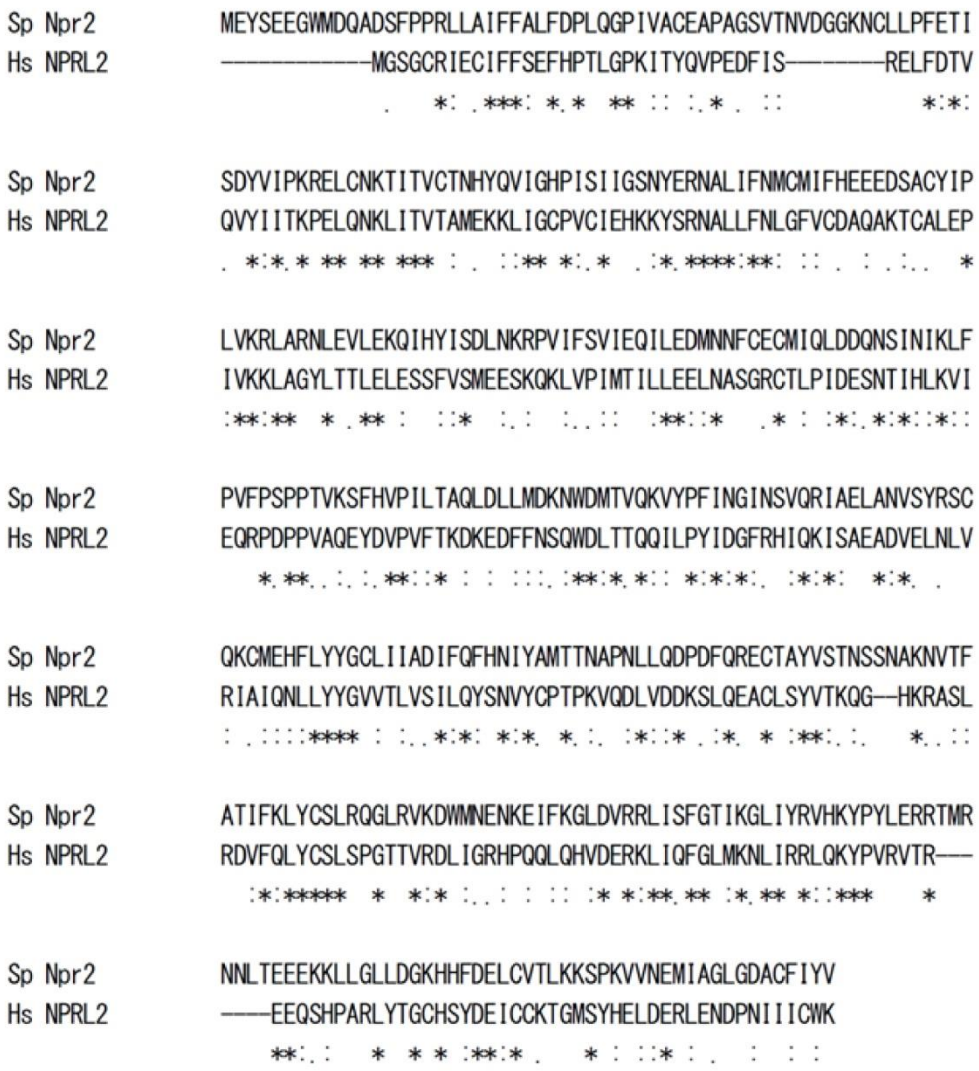

Figure S1 Alignment of protein sequences of *Schizosaccharomyces pombe* (Sp) Npr2 with related proteins from humans (Hs) NPRL2. Sequence alignment was performed using the CLUSTALW program. Asterisks indicate identical amino acids, colons indicate strictly conserved amino acids and dots indicate conserved amino acids.

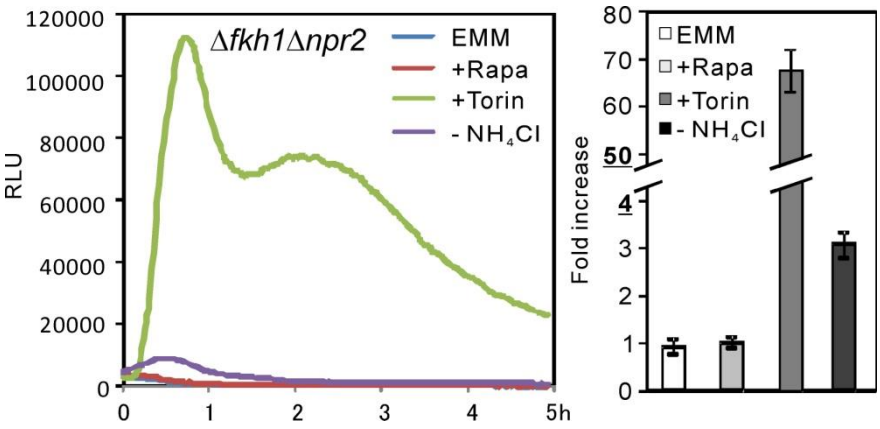

Figure S2 The *fkh1* deletion abolished rapamycin-induced reporter activity in Δ*npr2* cells. The Δ*fkh1*Δ*npr2* cells harboring the reporter vector pKB8527 were grown to exponential phase, and assayed as described in Figure 4A. Standard deviations of ratio are from three independent experiments, and each sample was analyzed in triplicate.

Table S1 Fission yeast strains used in this study

Strain	Genotype	Reference
HM123	*h⁻ leu1-32*	Our stock
KP456	*h⁻ leu1-32 ura4-D18*	Our stock
KP928	*h⁺ his2 leu1-32 ura4-D18*	Our stock
KP207	*h⁺ his2 leu1-32*	Our stock
KP91087	*h⁺ leu1-32 ade6 ura4-D18 tsc2*::*KanMX₄*	(KIM *et al.* 2010)
KP90390	*h⁺ leu1-32 ade6 ura4-D18 npr2*::*KanMX₄*	(KIM *et al.* 2010)
KP93006	*h⁺ leu1-32 ade6 ura4-D18*	(KIM *et al.* 2010)
KP5131	*h⁻ leu1-32 tsc2*::*KanMX₄*	This study
KP5236	*h⁺ leu1-32 npr2*::*KanMX₄*	This study
KP5080	*h⁻*	This study
KP5128	*h⁻ tsc2*::*KanMX₄*	This study
KP5237	*h⁻ npr2*::*KanMX₄*	This study
KP5395	*h⁻ ura4-D18 tsc2*::*ura4⁺*	(MATSUMOTO *et al.* 2002)
KP5482	*h⁻ leu1-32 tor2-287*	(HAYASHI *et al.* 2007)
KP5734	*h⁺ tor2-287*	This study
KP5637	*h⁺ tor2-287 tsc2*::*KanMX₄*	This study
KP5579	*h⁺ tor2-287 npr2*::*KanMX₄*	This study
KP5875	*h⁻ tor2^{S1837E}*:*KanMX*	(NAKASHIMA *et al.* 2010)
KP5873	JUP1350 *h^{90} tor2^{L1310P}*:*KanMX*	(URANO *et al.* 2007)
KP5874	JUP1352 *h^{90} tor2^{E2221K}*:*KanMX*	(URANO *et al.* 2007)

KP5490	*h⁺ura4-D18 tsc2*::*ura4⁺ npr2*::*KanMX₄*	This study
KP5750	*h⁻ leu1-32 ura4-D18 cat1*::*ura4⁺*	This study
KP6029	*h⁻ ura4-D18 cat1*::*ura4⁺ tsc2*::*KanMX₄*	This study
KP6031	*h⁺ ura4-D18 cat1*::*ura4⁺ npr2*::*KanMX₄*	This study
KP6033	*h⁺ ura4-D18 tor2-287 cat1*::*ura4⁺*	This study
KP6034	*h⁺ ura4-D18 cat1*::*ura4⁺*	This study
KP2233	*h⁺ leu1-32 his2 ura4-D18 fkh1*::*ura4⁺*	(SIO *et al.* 2005)
KP5585	*h⁻ leu1-32 ura4-D18 fkh1*::*ura4⁺ npr2*::*KanMX₄*	This study
KP5855	*h⁻ leu1-32 ura4-D18 tsc2*::*ura4⁺ npr2*::*KanMX₄*	This study
KP5859	*h⁺ ura4-D18 Cat1-GFP:ura4⁺*	This study
KP5822	*h⁺ ura4-D18 npr2*::*KanMX₄ Cat1-GFP:ura4⁺*	This study
KP5826	*h⁺ura4-D18 tsc2*::*KanMX₄ Cat1-GFP:ura4⁺*	This study
KP5955	*h⁺ ura4-D18 tor2-287 Cat1-GFP:ura4⁺*	This study
KP5903	*h⁻ gtr1*::*KanMX₆*	(VALBUENA *et al.* 2012)
KP5904	*h⁻ ura4-D18 gtr2*::*ura4⁺*	(VALBUENA *et al.* 2012)
KP5914	*h⁺ ura4-D18 tor2-287*	This study
KP5968	*h⁺ ura4-D18 gtr2*::*ura4⁺ tor2-287*	This study
KP5974	*h⁺ ura4-D18 gtr2*::*ura4⁺ npr2*::*KanMX₄*	This study
KP6385	*h⁻ ura4-D18 tor2-287 npr2*::*KanMX₄ Cat1-GFP:ura4⁺*	This study
KP6366	*h⁻ npr2*::*natMX₆*	This study
KP6402	*h⁻ npr2*::*natMX₆ tor2^{S1837E}*:*KanMX*	This study

HAYASHI, T., M. HATANAKA, K. NAGAO, Y. NAKASEKO, J. KANOH *et al.*, 2007 Rapamycin sensitivity of the *Schizosaccharomyces pombe tor2* mutant and organization of two highly phosphorylated TOR complexes by specific and common subunits. Genes Cells **12:** 1357-1370.

KIM, D. U., J. HAYLES, D. KIM, V. WOOD, H. O. PARK *et al.*, 2010 Analysis of a genome-wide set of gene deletions in the fission yeast *Schizosaccharomyces pombe*. Nat Biotechnol **28:** 617-623.

MATSUMOTO, S., A. BANDYOPADHYAY, D. J. KWIATKOWSKI, U. MAITRA and T. MATSUMOTO, 2002 Role of the Tsc1-Tsc2 complex in signaling and transport across the cell membrane in the fission yeast *Schizosaccharomyces pombe*. Genetics **161:** 1053-1063.

NAKASHIMA, A., T. SATO and F. TAMANOI, 2010 Fission yeast TORC1 regulates phosphorylation of ribosomal S6 proteins in response to nutrients and its activity is inhibited by rapamycin. J Cell Sci **123:** 777-786.

SIO, S. O., T. SUEHIRO, R. SUGIURA, M. TAKEUCHI, H. MUKAI *et al.*, 2005 The role of the regulatory subunit of fission yeast calcineurin for *in vivo* activity and its relevance to FK506 sensitivity. J Biol Chem **280:** 12231-12238.

URANO, J., T. SATO, T. MATSUO, Y. OTSUBO, M. YAMAMOTO *et al.*, 2007 Point mutations in TOR confer Rheb-independent growth in fission yeast and nutrient-independent mammalian TOR signaling in mammalian cells. Proc Natl Acad Sci U S A **104:** 3514-3519.

VALBUENA, N., K. L. GUAN and S. MORENO, 2012 The Vam6 and Gtr1-Gtr2 pathway activates TORC1 in response to amino acids in fission yeast. J Cell Sci **125:** 1920-1928.

Table S2 Binding of Npr2 with components of the SEA complex in fission yeast

Budding yeast gene	Homolog in fission yeast	Product	Binding with Npr2
SEH1	SPAC15F9.02	nucleoporin Seh1	ND
SEA1/IML1	SPBC26H8.04c	DEP domain protein, human DEPDC5 ortholog	+
SEA2	SPAC4F8.11	WD repeat protein, human WDR24 family	+
SEA3	SPAC11E3.05	ubiquitin-protein ligase E3, human WDR59 ortholog	+
SEA4	SPAC12G12.01c/ SPAC630.02	ubiquitin-protein ligase E3	+
NPR3	SPBC543.04/Npr3	Npr2/3 complex subunit Npr3	+

ND indicates not determined.

+ indicates the binding with Npr2 was demonstrated based on the *S. pombe* predicted protein interaction database (www.bahlerlab.info/PInt).